Radiative effects in deep inelastic scattering of polarized leptons by polarized light nuclei

1994 J. Phys. G: Nucl. Part. Phys. 20 513

(http://iopscience.iop.org/0954-3899/20/4/001)

J. Phys. G: Nucl. Part. Phys. 20 (1994) 513–531. Printed in the UK

Radiative effects in deep inelastic scattering of polarized leptons by polarized light nuclei

I V Akushevich and N M Shumeiko

National Scientific and Education Center of Particle and High Energy Physics attached to Byelorussian State University, 220040 Minsk, Belarus

Received 25 August 1993, in final form 30 Novembwer 1993

Abstract. Principal contributions to QED radiative effects in deep inelastic scattering (DIS) of polarized leptons by polarized targets (H, D, ^{3}He) are investigated both on the Born level and taking into account radiative corrections (RC). Scattering in the case of transverse polarized targets is also considered. All quantities are presented in terms of covariant variables. Exact results are obtained for low-order corrections. Detailed numerical analysis under the conditions of forthcoming polarization experiments is carried out. Two points of view on calculation of RC to experimental data are discussed in detail. The results of a computer run in the regime of data-processing iteration procedure are presented.

1. Introduction

Recent measurements of the spin-dependent polarized proton structure function (SF) $g_1^p(x)$ [1] and a test of the Ellis–Jaffe sum rule [2] renewed an interest to the problem of internal spin structure of the nucleon. The experimental results considered in the naive quark–parton model show that only a small part of the proton spin is carried by the valence quarks. This unexpected result has led to numerous speculations and suggestions concerning the proton spin theory (see [3] and references therein). There are only a few measurements for the spin-dependent SF of the proton [1, 4] and no data for the second-proton spin-dependent SF $g_2^p(x)$. Recently data on the neutron SF $g_1^n(x)$ were obtained by SMC collaboration at CERN [5] and at SLAC (experiment E142) [6]. Measurements of the SF would provide a verification of Burkhardt–Cottingham [7] and especially Bjorken [8] sum rules. New experiments are also planned at accelerator complexes HERA (HERMES [9]), UNK [10] and FNAL [11]. Apart from the additional data for $g_1^p(x)$ and $g_1^n(x)$, the implementation of transverse-polarized targets will produce data sets for $g_2^p(x)$.

The interpretation of the experimental data requires a correct calculation of radiative corrections (RC). In this article we consider the inclusive DIS processes of polarized charged leptons by polarized light nuclei (H, D, ^{3}He), taking into account radiative effects. The covariant method for the RC calculation, offered by Bardin and Shumeiko in [12, 13] and developed in [14–16] is used.

It is well known that there are three channels of scattering of virtual photon by a nucleus, in dependence on transfer energy $\nu = E_1 - E_2$, where E_1 (E_2) is the initial (scattered) lepton energy: elastic, quasielastic or inelastic. A representative plot of the scattering cross section as a function of ν and square of transfer momentum $Q^2 = -q^2$ is shown on figure 1. The peak in the range I (for $\nu = 0$, if we neglect nuclear recoil) corresponds to elastic scattering.

0954-3899/94/040513+19$19.50

In this case the nucleus remains in the ground state. Range II takes up quasielastic scattering, i.e. direct collisions of leptons with nucleons inside nucleus. Wide maximum in the energy spectrum originates from the movement of nucleons. Range III of inelastic scattering occurs when transfer energy is greater then the pion threshold. Only the contributions which will be discussed below are indicated in figure 1. Contributions of other collective nuclear effects such as coherent nuclear level excitation and scattering from clusters within the nucleus are usually neglected when RC are considered (see e.g. [17]). Detailed discussion of the contributions to the lepton scattering on nuclei can be found in literature (see reviews [18–21]).

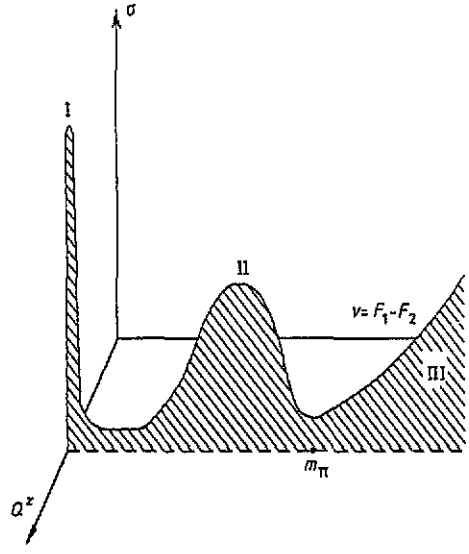

Figure 1. The double differential cross section of the inclusive lepton–nuclei scattering as a function of ν and Q^2 (arbitrary scale).

Both ν and Q^2 are fixed by kinematics at the Born level. Hence, the channel of scattering is fixed as well. In this article we discuss inelastic scattering experiments. However, the uncertainty of the radiated real-photon momentum takes away the fixation of the quantities ν and Q^2 on a level of RC and each of the three channels contributes to the cross section. Integration over the photon phase space leads to that in a plane of ν and Q^2. Adding a virtual photon contribution σ_v, we have for the lowest-order RC

$$\sigma = \sigma_{in} + \sigma_{el} + \sigma_q + \sigma_v. \tag{1}$$

Each σ denotes the double differential cross section $d^2\sigma/dxdy$, and x, y are usual scaling nucleon variables. σ_{in}, the contribution of radiative tail from continuous spectrum (IRT), is calculated explicitly in the article. The contribution of radiative tail from elastic peak (ERT) σ_{el} must be expressed in terms of elastic form factors and can be obtained from σ_{in} by the substitution such as (27)–(29) and by multiplying on a factor containing $\delta(\nu - Q^2/2M)$, M being the target mass. The explicit result is also presented. The contribution of the radiative tail from the quasielastic scattering (QRT) σ_q can be obtained from the formulae for the one-nucleon ERT with the form factors corrected by a suppression factor (see e.g. [22]).

The paper is organized as follows. In section 2 we present the results necessary for constructing the observable quantities. The hadronic tensor (4) for spin-1 particles in the case of the DIS of polarized particles is obtained on the basis of covariant spin-1 density matrix and the results of [23]. Here we also show how to obtain the hadronic tensors in the case of DIS on spin-1/2 and spin-0 particles from (4). By analogy with [24], the covariant representation for polarization vectors for longitudinally and transversely polarized targets

is given in appendix A. The Born cross section of DIS of polarized charged leptons on spin-1 target is studied in section 3. Both exact, that is, involving no approximation in the framework of the considered order of perturbation theory, and ultrarelativistic formulae are presented. Exact infrared-free formulae for the next-to-Born order are obtained in section 4. Here we also discuss a calculation method inasmuch as it slightly differs from the one maintained in [13–15]. The most cumbersome expressions of the final exact formulae are collected in appendix B. Section 5 is devoted to the discussion of the numerical results obtained under the conditions of the forthcoming polarized DIS experiments. We represent our FORTRAN program POLRAD created on the basis of exact formulae for RC. The results of POLRAD running in the regime of the data processing iteration procedure are discussed. Besides, section 5 contains a detailed discussion of the experimental fits and models for SF and form factors. Two versions for the RC procedure of experimental data are also discussed.

2. The hadronic tensor

DIS on polarized spin-1 target in the Born approximation was considered in [23] (see also [25, 26]). We use the hadronic tensor from [23] and construct the density matrix for a spin-1 particle in accordance with [27] (see also [28])†

$$\rho_{\mu\nu}(p) = \frac{1}{3} I_{\mu\nu}(p) - \frac{\mathrm{i} P_N}{2M} \epsilon_{\mu\nu\alpha\beta} p_\alpha \eta_\beta + \frac{Q_N}{6} \left(I_{\mu\nu}(p) - 3\eta_\mu \eta_\nu \right) \tag{2}$$

where

$$I_{\mu\nu}(p) = -g_{\mu\nu} + p_\mu p_\nu / M^2. \tag{3}$$

Also, $P_N = \beta^+ - \beta^-$ and $Q_N = \beta^+ + \beta^- - 2\beta^0 = 1 - 3\beta^0$ define polarization and quadrupolarization degrees, respectively; β^+, β^-, β^0 are the relative numbers of particles with the corresponding spin projections on a direction n, and η is the covariant representation (see appendix A) of n. In what follows, it is referred to as the polarization vector of a target. We give a detailed description of the beam and target polarization vector in appendix A.

The hadronic tensor in the form convenient for RC calculations is

$$\begin{aligned} W_{\mu\nu} = & -\tilde{g}_{\mu\nu} \left(F_1 + \frac{Q_N}{6} b_1 \right) + \frac{\tilde{p}_\mu \tilde{p}_\nu}{pq} \left(F_2 + \frac{Q_N}{6} b_2 \right) \\ & + \mathrm{i} M P_N \left(\frac{\epsilon_{\mu\nu\alpha\beta} q_\alpha \eta_\beta}{pq} (g_1 + g_2) - \frac{\epsilon_{\mu\nu\alpha\beta} q_\alpha p_\beta (q\eta)}{(pq)^2} g_2 \right) \\ & + \frac{M^2}{pq} \frac{Q_N}{6} \left(\tilde{g}_{\mu\nu} k_n b_1 - \frac{\tilde{p}_\mu \tilde{p}_\nu}{pq} k_n \left(\frac{b_2}{3} + b_3 + b_4 \right) \right. \\ & \left. - (\tilde{g}_{\mu\nu} + 3\tilde{\eta}_\mu \tilde{\eta}_\nu) \left(\frac{b_2}{3} - b_3 \right) - \frac{3}{2} \frac{M^2}{pq} \tilde{\Omega}_{\mu\nu} \left(\frac{b_2}{3} - b_4 \right) \right) \end{aligned} \tag{4}$$

where q is the virtual photon 4-momentum,

$$\begin{aligned} k_n &= \frac{3(q\eta)^2 - Q^2}{pq} \qquad & \tilde{\Omega}_{\mu\nu} &= \frac{(\tilde{p}_\mu \tilde{\eta}_\nu + \tilde{\eta}_\mu \tilde{p}_\nu) q\eta}{M^2} \\ \tilde{g}_{\mu\nu} &= g_{\mu\nu} + \frac{q_\mu q_\nu}{Q^2} & \tilde{p}_\mu &= p_\mu + \frac{pq}{Q^2} q_\mu \qquad \tilde{\eta}_\mu = \eta_\mu + \frac{\eta q}{Q^2} q_\mu. \end{aligned} \tag{5}$$

† Equation (2) can be obtained from the general covariant density matrix [27] when spin functions are the eigenvectors of the spin projection operator. This corresponds to the considered experimental situation (see the review by Lapidus [28]).

The tensor $W_{\mu\nu}$ (4) can be recast to a form

$$W_{\mu\nu}(p,q) = \rho_{\alpha\beta}(p) T^{\alpha\beta}_{\mu\nu}(p,q) \tag{6}$$

where the tensor $T^{\alpha\beta}_{\mu\nu}(p,q)$ does not depend on any polarization characteristics and generally can be represented in the form (5) of [25]. A hadronic tensor for elastic scattering (or ERT) can also be recast to this form. Therefore, we can obtain the expressions for SF appearing in (4) via elastic form factors of a vector particle. The explicit forms of the expressions are given in section 4.

We note that the hadronic tensor for spin-1/2 particle is derived from (4) by putting $Q_N = 0$. The formulae for the covariant representation of polarization vectors are also valid in this case. The hadronic tensor for scalar particles is derived by $P_N = Q_N = 0$.

3. The Born approximation

Using (4) for the DIS cross section on the Born level, we obtain

$$\begin{aligned}\frac{\mathrm{d}^2\sigma}{\mathrm{d}x\,\mathrm{d}y} = \frac{4\pi\alpha^2}{\sqrt{\lambda_s}}\frac{S_x}{Q^4}\Bigg\{&(Q^2-2m^2)\left[F_1 + \frac{Q_N}{6}(1+k_n\epsilon)b_1\right]\\ &+\frac{SX-M^2Q^2}{S_x}\left[F_2+\frac{Q_N}{6}\left(b_2+k_n\epsilon\left(\frac{b_2}{3}+b_3+b_4\right)\right)\right]\\ &+\frac{mM}{S_x}P_N\left[(Q^2\,\xi\eta - q\eta\, k_2\xi)(g_1+g_2)+(k_2\xi - 2\,\xi p\; Q^2/S_x)q\eta\; g_2\right]\\ &-\frac{Q_N}{12}\epsilon\Bigg[(Q^2+4m^2+12\eta k_1\;\eta k_2)\left(\frac{b_2}{3}-b_3\right)\\ &-\frac{3q\eta}{S_x}(X\eta k_1 + S\eta k_2)\left(\frac{b_2}{3}-b_4\right)\Bigg]\Bigg\}.\end{aligned} \tag{7}$$

Here $k_1(k_2)$, ξ, m are the initial (final) lepton's momentum, polarization vector and mass, respectively and $\epsilon = M^2/pq = 2M^2/S_x$. Invariants are defined in a standard way in (A.3). Equality (7) is true for the any direction of polarization vectors and is exact: no approximations were made yet. The exact formulae for the DIS cross section of longitudinal polarized leptons on longitudinal and transverse polarized nuclei can be obtained by using (7) and the explicit form of polarization vectors from appendix A.

By applying the ultrarelativistic approximation

$$m^2, M^2 \ll S, X, Q^2 \qquad \xi = P_L k_1/m \tag{8}$$

and transferring to scaling variables x and y, we further find

$$\frac{\mathrm{d}^2\sigma}{\mathrm{d}x\,\mathrm{d}y} = \frac{4\pi\alpha^2 S}{Q^4}\left[\left(F_1 - \frac{Q_N}{3}b_1\right)xy^2 + \left(F_2 - \frac{Q_N}{3}b_2\right)(1-y) - P_L P_N xy(2-y)g_1\right] \tag{9}$$

in the case of a longitudinal polarized target and

$$\begin{aligned}\frac{\mathrm{d}^2\sigma}{\mathrm{d}x\,\mathrm{d}y} = \frac{4\pi\alpha^2 S}{Q^4}\Bigg[&\left(F_1 + \frac{Q_N}{6}b_1\right)xy^2 + \left(F_2 + \frac{Q_N}{6}b_2\right)(1-y)\\ &-2P_L P_N \frac{x\sqrt{xy(1-y)}M}{\sqrt{S}}(yg_1 + 2g_2)\Bigg]\end{aligned} \tag{10}$$

for a transverse one. P_L is the polarization lepton degree.

The formulae of section 6 of [23] can be easily obtained from (9) and (10). It is necessary to use $P_L = 0$, the Callan–Gross relations $F_2 = 2xF_1$ and $b_2 = 2xb_1$, and to

choose Q_N for a pure state: $Q_N = \pm 1$ and $Q_N = -2$ for states with the spin projection H equal to ± 1 and 0, respectively.

4. Exact results for radiative corrections

The phase-space element of the photon was shown in [14] to be expressed in the form

$$\int \frac{\mathrm{d}^3 k}{k_0} = \int \mathrm{d}M_x^2 \int \mathrm{d}t \int \frac{\mathrm{d}z_2}{\sqrt{R_z}} \tag{11}$$

where $R_z = A_z z_2^2 + 2B_z z_2 - C_z$, M_x is the invariant mass of the final hadrons and $z_{1(2)} = 2kk_{1(2)}$. Designation and explicit form of the functions A_z, B_z, C_z can be found in [12–14]. The integrand admits analytical integration over z_2 because it does not contain this variable in SF arguments. After the integration and a transformation of the integrand variable, the contribution of IRT can be ortained in the form

$$\sigma_{\mathrm{in}} = -\frac{\alpha^3 S_x}{\lambda_s^{1/2}} \int_{\tau_{\min}}^{\tau_{\max}} \mathrm{d}\tau \sum_{i=1}^{8} \sum_{j=1}^{k_i} \theta_{ij}(\tau) \int_0^{R_{\max}} \mathrm{d}R \frac{R^{j-2}}{t^2} \Im_i(R, \tau). \tag{12}$$

where the quantities $\Im_i$ are defined as some combinations of SF

$$\begin{aligned}
&\Im_1 = F_1 + \frac{Q_N}{6} b_1 && \Im_2 = \epsilon \left(F_2 + \tfrac{Q_N}{6} b_2 \right) \\
&\Im_3 = P_N \epsilon (g_1 + g_2) && \Im_4 = P_N \epsilon^2 g_2 \\
&\Im_5 = \frac{Q_N}{6} \epsilon^2 b_1 && \Im_6 = \frac{Q_N}{6} \epsilon^3 (b_2/3 + b_3 + b_4) \\
&\Im_7 = \frac{Q_N}{6} \epsilon (b_2/3 - b_3) && \Im_8 = \frac{Q_N}{6} \epsilon^2 (b_2/3 - b_4).
\end{aligned} \tag{13}$$

Summation over $i = 1, \ldots, 8$ corresponds to the contributions of various $\Im_i$,

$$\begin{aligned}
&R = W^2 - M_x^2 - t + Q^2 && \tau = (t - Q^2)/R \\
&R_{\max} = \frac{W^2 - (M + m_\pi)^2}{1 + \tau} && \tau_{\max,\min} = \frac{S_x \pm \sqrt{\lambda_Q}}{2M^2} \\
&\lambda_Q = S_x^2 + 4M^2 Q^2 && W^2 = S_x - Q^2 + M^2 \\
&t = -(k_1 - k - k_2)^2 = Q^2 + R\tau && \epsilon = M^2/pq = 2M^2/(S_x - R).
\end{aligned} \tag{14}$$

R and τ are separated in the expression for the results of the analytical integration over z_2,

$$\int \mathrm{d}z_2 \frac{A_i(z_2)}{\sqrt{R_z}} = \frac{\theta_{i1}(\tau)}{R} + \theta_{i2}(\tau) + R\theta_{i3}(\tau) + R^2 \theta_{i4}(\tau) \tag{15}$$

where $A(z_2)$ contains not only expressions of the type

$$z_1^{-1}, z_2^{-1}, z_1^{-2}, z_2^{-2}, z_1, z_2, \ldots \tag{16}$$

but also scalar multiplications $k\xi$, $k\eta$, which, however, are reduced to (16) after substitution of the explicit form for ξ and η from appendix A. Summation over j corresponds to expansion (15), and j runs from 1 to k_i which take the values

$$k_i = (3, 3, 4, 5, 5, 5, 3, 4) \tag{17}$$

for various i. Explicit forms of functions $\theta_{ij}(\tau)$ are given in appendix B.

The infrared divergence occurs in the integral for $R \to 0$ in the term with $j = 1$ (and only in it) and is cancelled by adding of the virtual photon contribution. For the infrared-free sum of σ_v and σ_{in} we find

$$\sigma_v + \sigma_{in} = \frac{\alpha}{\pi}(\delta_R^{IR} + \delta_{vert} + \delta_{vac}^l + \delta_{vac}^h)\sigma_0 + \sigma_{in}^F. \tag{18}$$

σ_{in}^F is the infrared free part of the IRT cross section

$$\sigma_{in}^F = -\frac{\alpha^3 S_x}{\lambda_s^{1/2}} \int_{\tau_{min}}^{\tau_{max}} d\tau \sum_{i=1}^{8} \left\{ \theta_{i1}(\tau) \int_0^{R_{max}} \frac{dR}{Rt} \left[\frac{\Im_i(R,\tau)}{t} - \frac{\Im_i(0,0)}{Q^2} \right] \right.$$
$$\left. + \sum_{j=2}^{k_i} \theta_{ij}(\tau) \int_0^{R_{max}} dR \frac{R^{j-2}}{t^2} \Im_i(R,\tau) \right\}. \tag{19}$$

δ_R^{IR} appears when the infrared divergence is extracted from σ_{in} using the Bardin–Shumeiko method. The virtual photon contribution consists of the lepton vertex correction δ_{vert} and the vacuum polarization by leptons δ_{vac}^l and hadrons δ_{vac}^h. For completeness we give the explicit form to δ_R^{IR}, δ_{vert} and δ_{vac}^l (the fit for $\delta_{vac}^h(Q^2)$ was taken from [29]),

$$\delta_{vert} = J_0 \ln\frac{\lambda}{m} + \left(\frac{3}{2}Q^2 + 4m^2\right)L_m - 2 - \frac{Q_m^2}{\sqrt{\lambda_m}}\left(\frac{1}{2}\lambda_m L_m^2 + 2\Phi\left(\frac{2\sqrt{\lambda_m}}{Q^2+\sqrt{\lambda_m}}\right) - \frac{\pi^2}{4}\right) \tag{20}$$

where λ is the photon mass, $\Phi(x)$ is the Spence function, $J_0 = 2(Q_m^2 L_m - 1)$, $\lambda_m = Q^4 + 4m^2Q^2$, $L_m = \lambda_m^{-1/2}\ln[(\sqrt{\lambda_m} + Q^2)/(\sqrt{\lambda_m} - Q^2)]$ and

$$\delta_{vac}^l = \sum_{i=e,\mu,\tau}\left[\frac{2}{3}(Q^2 + 2m_i^2)L_m^i - \frac{10}{9} + \frac{8m_i^2}{3Q^2}(1 - 2m_i^2 L_m^i)\right]. \tag{21}$$

The quantity L_m^i is obtained from L_m by a substitution $m \to m_i$.

$$\delta_R^{IR} = J_0 \ln\frac{W^2 - (M+m_\pi)^2}{\lambda\sqrt{W^2}} + \tfrac{1}{2}(S'L_{S'} + X'L_{X'}) + S_\phi(Q_m^2, \lambda_m, a', b') \tag{22}$$

where [15]

$$S' = X + Q^2 \qquad X' = S - Q^2$$
$$\lambda_{S'} = S'^2 - 4W^2m^2 \qquad \lambda_{X'} = X'^2 - 4W^2m^2$$
$$L_{S'} = \frac{1}{\sqrt{\lambda_{S'}}}\ln\frac{S' + \sqrt{\lambda_{S'}}}{S' - \sqrt{\lambda_{S'}}} \qquad L_{X'} = \frac{1}{\sqrt{\lambda_{X'}}}\ln\frac{X' + \sqrt{\lambda_{X'}}}{X' - \sqrt{\lambda_{X'}}} \tag{23}$$
$$a' = \frac{1}{2W^2}(SX - M^2Q^2 - W^2(Q^2 + 4m^2))$$
$$b' = \frac{1}{W^2}(Q^2(SX - M^2Q^2) - m^2\lambda_Q)).$$

In the article we use the function S_ϕ in the form originally obtained and adduced in an old and rare preprint [12] only†:

$$S_\phi(s,\lambda,a,b) = \frac{s}{2\sqrt{\lambda}}\sum_{i=1}^{2}(-1)^i\sum_{j=1}^{4}\delta_j\sum_{k=1}^{2}\left[\Phi\left(\frac{\gamma_i - \gamma}{\gamma_i - \gamma_k^j}\right) + \Phi\left(\frac{\gamma + (-1)^i}{\gamma_k^j + (-1)^i}\right)\right]\Bigg|_{\gamma_l}^{\gamma_u} \tag{24}$$

† Another form of S_ϕ has been reported in [13, equations (57), (58)] and [12, equation (12)]; also, S_ϕ from [15], which equals that in equation (24), is obtained from equations (57), (58) of [13] with a substitution $M^2 \to W^2$, which should be done when DIS is considered.

where

$$\delta_j = (1, 1, -1, -1) \qquad \gamma_{1,2} = \mp\frac{(\sqrt{b} \mp \sqrt{\lambda})^2}{b-\lambda}$$

$$\gamma_{1,2}^j = -(a_j\sqrt{b} \pm \sqrt{ba_j^2 + \tau_j^2})/\tau_j \qquad \gamma_u = (\sqrt{b+\lambda} - \sqrt{b})/\sqrt{\lambda} \tag{25}$$

$$a_j = s - \delta_j\sqrt{\lambda} \qquad \tau_j = -a\sqrt{\lambda} + \tfrac{1}{2}\delta_j(b-\lambda) + (-1)^j\sqrt{D}$$

$$D = (s+a)(\lambda a - sb) + \tfrac{1}{4}(\lambda + b)^2.$$

We note that the compact form of S_ϕ in the ultrarelativistic approximation (equation (13) of [15]) is often more suitable.

In the case of ERT the cross section can be obtained from (12) by an appropriate substitution of some quadratic combinations of form factors for SF and by a trivial integration over R using a δ-function $\delta(R - R_{\rm el})$, where $R_{\rm el} = (S_x - Q^2)/(1+\tau)$. As a result we have for $\sigma_{\rm el}$

$$\sigma_{\rm el} = \frac{1}{A}\frac{{\rm d}^2\sigma_{\rm el}}{{\rm d}x_A{\rm d}y} = -\frac{\alpha^3 S_x}{\lambda_s^{1/2}}\int_{\tau_{\min}}^{\tau_{\max}} {\rm d}\tau \sum_{i=1}^{8}\sum_{j=1}^{k_i}\theta_{ij}(\tau)\frac{2M_A^2 R_{\rm el}^{j-2}}{(1+\tau)t^2}\Im_i^{\rm el}(R_{\rm el}, \tau). \tag{26}$$

The invariants (A.3) appearing in (26) contain the nucleus momentum p_A instead of p ($p_A^2 = M_A^2$, M_A is the nucleus mass). The functions $\Im_i^{\rm el}(R_{\rm el}, \tau)$ are obtained from $\Im_i(R, \tau)$, defined in (12), (13), by switching from SF to form factors. The explicit form of the expression depends on the target spin. For the proton, such change was done in [16]. The following expressions should be used for the deuteron:

$$\Im_1^{\rm el} = \frac{1}{6}\eta_{\rm d}F_{\rm m}^2(4(1+\eta_{\rm d}) + \eta_{\rm d}Q_N)$$

$$\Im_2^{\rm el} = \left(F_{\rm c}^2 + \frac{2}{3}\eta_{\rm d}F_{\rm m}^2 + \frac{8}{9}\eta_{\rm d}^2F_{\rm q}^2\right) + \frac{Q_N}{6}\left(\eta_{\rm d}F_{\rm m}^2 + \frac{4\eta_{\rm d}^2}{1+\eta_{\rm d}}\left(\frac{\eta_{\rm d}}{3}F_{\rm q} + F_{\rm c} - F_{\rm m}\right)F_{\rm q}\right)$$

$$\Im_3^{\rm el} = -\frac{P_N}{2}(1+\eta_{\rm d})F_{\rm m}(\frac{\eta_{\rm d}}{3}F_{\rm q} + F_{\rm c})$$

$$\Im_4^{\rm el} = \frac{P_N}{4}F_{\rm m}\left(\frac{1}{2}F_{\rm m} - F_{\rm c} - \frac{\eta_{\rm d}}{3}F_{\rm q}\right) \tag{27}$$

$$\Im_5^{\rm el} = \frac{Q_N}{24}F_{\rm m}^2$$

$$\Im_6^{\rm el} = \frac{Q_N}{24}\left(F_{\rm m}^2 + \frac{4}{1+\eta_{\rm d}}\left(\frac{\eta_{\rm d}}{3}F_{\rm q} + F_{\rm c} + \eta_{\rm d}F_{\rm m}\right)F_{\rm q}\right)$$

$$\Im_7^{\rm el} = \frac{Q_N}{6}\eta_{\rm d}(1+\eta_{\rm d})F_{\rm m}^2$$

$$\Im_8^{\rm el} = -\frac{Q_N}{6}\eta_{\rm d}F_{\rm m}(F_{\rm m} + 2F_{\rm q}).$$

Here $\eta_{\rm d} = t/4M_d^2 = (Q^2 + R_{\rm el}\tau)/4M_d^2$, and $F_{\rm c}$, $F_{\rm m}$, $F_{\rm q}$ are the charge, the magnetic and quadrupole form factors of deuteron, and M_d is its mass. The definitions of the form factors are the same as in [30] (see also [31]). We also give the expressions for the case of arbitrary spin-1/2 nuclei ($\eta_A = t/4M_A^2$),

$$\Im_1^{\rm el} = Z^2\eta_A G_{\rm m}^2 \qquad \Im_2^{\rm el} = Z^2\frac{G_{\rm e}^2 + \eta_A G_{\rm m}^2}{1+\eta_A}$$

$$\Im_3^{\rm el} = \frac{P_N Z^2}{2}G_{\rm m}G_{\rm e} \qquad \Im_4^{\rm el} = \frac{P_N Z^2}{4}G_{\rm m}\frac{G_{\rm e} - G_{\rm m}}{1+\eta_A} \tag{28}$$

and for a scalar nucleus

$$\Im_2^{\mathrm{el}} = Z^2 F^2 \tag{29}$$

where Z is the nucleus charge. All but the indicated SF must be set equal to zero.

The cross sections for QRT can be obtained using the results for ERT on the proton:

$$\sigma_{\mathrm{q}} = \sigma_{\mathrm{el}}(G_{\mathrm{pM}} \to G_{\mathrm{qM}},\ G_{\mathrm{pE}} \to G_{\mathrm{qE}}) \tag{30}$$

where

$$G_{\mathrm{qE}}^2 = Z S_{\mathrm{E}} G_{\mathrm{pE}}^2 \qquad G_{\mathrm{qM}}^2 = (Z\mu_p^2 + N\mu_n^2) S_{\mathrm{M}} G_{\mathrm{pE}}^2. \tag{31}$$

As usual, we suggest for neutron the form factors $G_{\mathrm{E}}^{\mathrm{neut}} = 0$, $G_{\mathrm{M}}^{\mathrm{neut}} = \mu_n G_{\mathrm{E}}^{\mathrm{prot}}$; μ_p and μ_n are the proton and neutron magnetic moments, S_{E} and S_{M} are the electric and magnetic suppression factors which should be calculated within a nucleus model, and Z and N are the proton and neutron numbers of a nucleus. Note that results for the quasielastic scattering by polarized light nuclei at the Born level can be found in [32].

5. Numerical analysis

In this section we present the FORTRAN code POLRAD created on the basis of the exact formulae for the radiative tails that we considered in the previous section. The program calculates the lowest-order RC to DIS of polarized leptons by polarized nuclei. Contributions of high orders are taken into account by the procedure of exponentiation in accordance with [15]. Here we discuss four points: fits and models of SF and form factors, numerical results for RC in ranges of forthcoming polarization experiments, run of POLRAD in the regime of the iteration procedure of data processing and the procedure of radiative correction of experimental data.

(a) Fits and models for SF and form factors. For the RC calculation we need fits of SF in a whole region of varyiation of the integration variables. We describe below the solving of the problem within POLRAD for the fits of the unpolarized, polarized and quadrupole SF in turn.

For unpolarized SF the problem of choosing a fit was discussed in [34]. Generally, we follow this paper but some modern data analyses and fits are adopted. For F_2 we use a well known fit for small Q^2 region: a parametrization from [35] below the resonance region and that from [22] (Stein fit) otherwise. In the rest of the region, the NA-37 fit [36] is used. We extrapolate these fits into regions that are not important for the RC value. Thus the NA-37 fit is extrapolated into the region $W \approx M_p + m_\pi (Q^2 > 6GeV^2)$ and Stein fit, into the region of large W. All fits are joined together along the lines of intersections. For $R(x, Q^2)$ we use the Whitlow fit R^{1990} [37] which is true for the values of Q^2 greater than $0.3\,\mathrm{GeV}^2$. Below this level we use the same R as in the above-mentioned references [22, 36]. Such is the POLRAD version for the unpolarized SF of proton. In order to take into account the other nuclei we must choose fits for $F_2^{\mathrm{d}}/F_2^{\mathrm{p}}$, F_2^A/F_2^{d} and R^A. For modelling $F_2^{\mathrm{d}}/F_2^{\mathrm{p}}$ we joined together the Whitlow fit of the SLAC region [37], the NA-37 fit and the Stein fit for small Q^2 regions. $F_2^A(x, Q^2)$ for other nuclei is obtained taking into account nuclear effects, and R is considered to be A-independent (e.g. see the review [38]).

For our calculation the spin-dependent SF g_1^{n}, g_1^{d}, $g_1^{^3\mathrm{He}}$ and g_2 for all considered nuclei are necessary. The current version of POLRAD exploits the convolution expressions for g_1^{d}, $g_1^{^3\mathrm{He}}$ via $g_1^{\mathrm{p}}(x)$ and $g_1^{\mathrm{n}}(x)$ calculated for the Bonn wavefunction in accordance with [39]. The model of [40] modified in [41], being in agreement with the experimental data, is used

for the nucleon SF. The SF $g_2(x)$ are omitted, since they do not have the leading twist contribution [23].

Quadrupole SF b_1, b_2 should be taken into account for deuterons as spin-1 particles. They are related by the Callan–Gross equality

$$b_2(x) = 2xb_1(x) \tag{32}$$

and conform to a sum rule obtained in [42]. A model of [43] is used for them.

A standard parametrization of deuteron form factors in the non-relativistic momentum approximation is used (see [31] and references therein). This parametrization deviates from experimental data for large Q^2, but this region gives a negligible contribution to ERT. If necessary, various corrections to the fit (relativistic, meson exchange, quark degrees of freedom) can be taking into account [31]. For ^{3}He form factors we used Schiff's model for the Gaussian wavefunction [44]. Nucleon form factors are taken from [45]. Charge form factor for scalar nuclei can be found, for example, in [18] (see section 3.8).

The suppression factors for QRT for DIS by a deuteron target are calculated as in [22]. Using Bernabeu model [46] gives practically the same numerical results. For other nuclei we used the Fermi gas model [20, 47].

(b) Numerical results for RC. We introduce the polarization asymmetry for a spin-1/2 target

$$A_{\mathrm{p}} = \frac{\sigma(\uparrow\uparrow) - \sigma(\uparrow\downarrow)}{\sigma(\uparrow\uparrow) + \sigma(\uparrow\downarrow)} \tag{33}$$

and polarization and quadrupolarization asymmetries for a spin-1 target

$$\begin{aligned} A_{\mathrm{p}} &= \frac{3}{2}\frac{\sigma(\uparrow\uparrow) - \sigma(\uparrow\downarrow)}{\sigma(\uparrow\uparrow) + \sigma(\uparrow\downarrow) + \sigma(\uparrow 0)} \\ A_{\mathrm{q}} &= \frac{1}{2}\frac{\sigma(\uparrow\uparrow) + \sigma(\uparrow\downarrow) - 2\sigma(\uparrow 0)}{\sigma(\uparrow\uparrow) + \sigma(\uparrow\downarrow) + \sigma(\uparrow 0)}. \end{aligned} \tag{34}$$

The arrows show the polarization of the lepton and the target, respectively. Following the tradition, we consider the spin asymmetry $A_1 = A_{\mathrm{p}}/D$ (A_1^{B} denotes the Born spin asymmetry) instead of polarization asymmetry. D is the kinematic depolarization factor.

The numerical analysis of the asymmetries in the range of small x is of great interest for the forthcoming polarization experiments. Figures 2 and 3 show the Born spin asymmetry and the spin asymmetry taking into account the radiative effects for proton and deuteron targets in the kinematics conditions of HERMES. Results for both longitudinal and transverse polarized targets are given. We also give results (figures 4 and 5) for longitudinally polarized targets at SMC and SLAC. The deuteron asymmetry is small for $x \leqslant 0.1$. Contributions of RC prevail in the region. This fact is illustrated in figure 6.

The greatest contribution to the total RC is given by the IRT. However, ERT for the proton and QRT for the deuteron and helium-3 dominate in the following cases: for $y \to 1$ in the ranges where $g_1(x) \approx 0$ ($x \approx 0.1$ for deuteron target, and when $x \to 0$) and in the case of transverse polarized targets. This fact is of special interest for more attractive range of small x because it corresponds to large y ($y > 0.7$). The contribution of σ_{v} to RC of the polarization asymmetry—but not to the cross section—is small.

The x dependence of the quadrupolarization asymmetry is presented in figure 7. It is less then 1%, owing to the smallness of b_1. ERT is independent of b_1- and dominates for small x.

(c) Iteration procedure of data processing. Data processing can be effected within the iteration procedure. We consider one of the simplest variants of the iteration procedure for

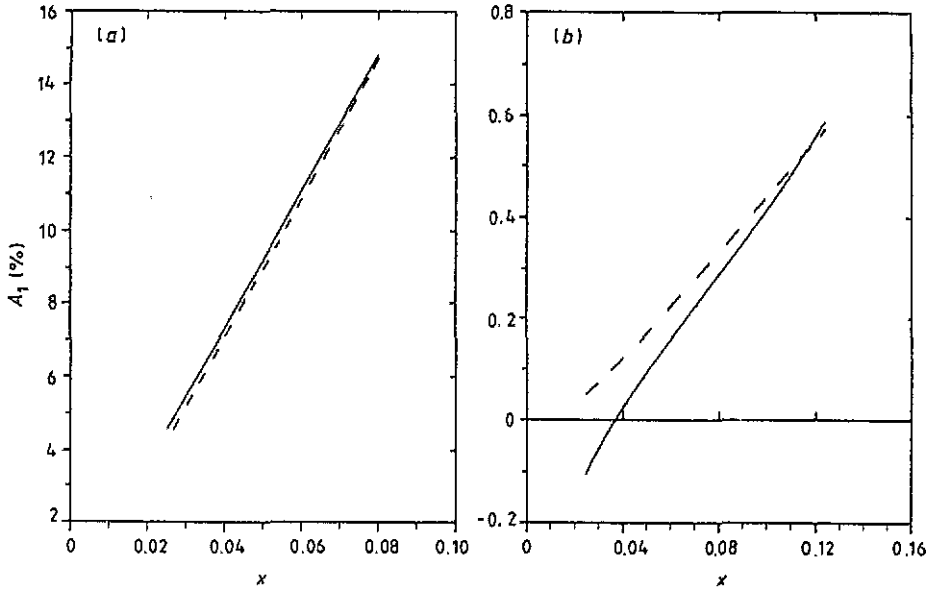

Figure 2. The x-dependence of the Born asymmetry (dashed line) and observed asymmetry (solid line) in the polarization electron–proton scattering for HERMES kinematics. $E = 35$ GeV. (*a*) Longitudinally polarized target, (*b*) transversely polarized target. The EMC fit [1] is used for g_1.

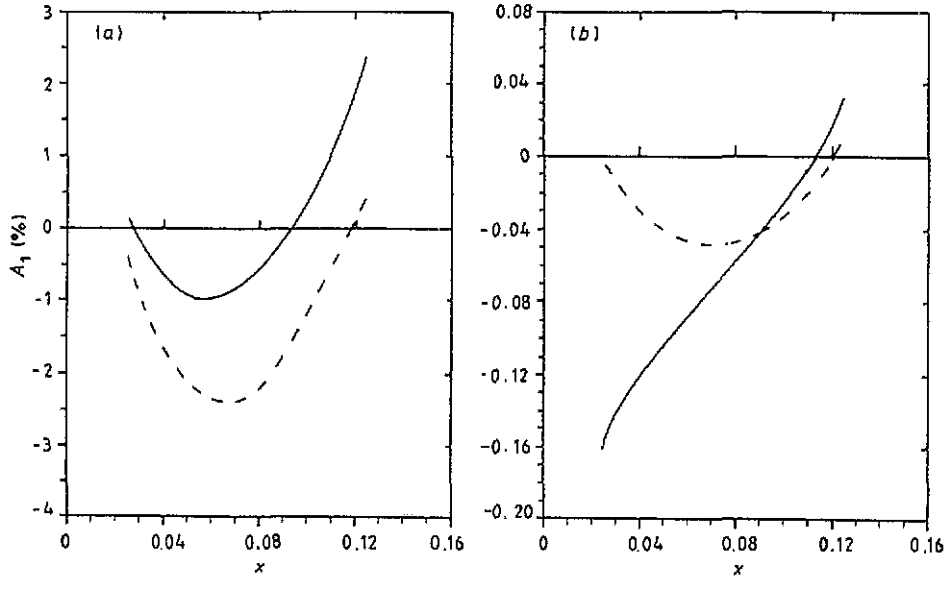

Figure 3. The x-dependence of the Born asymmetry (dashed line) and observed asymmetry (solid line) in the polarization electron–deuteron scattering for HERMES kinematics. $E = 35$ GeV. (*a*) Longitudinally polarized target, (*b*) transversely polarized target.

the spin asymmetry when only $g_1(x)$ is extracted, $g_2(x)$ equals 0 and the target (proton or deuteron) is longitudinally polarized. In this case we have for the observed spin asymmetry

$$A_{\mathrm{m}} = \frac{2xg_1(x)(1+R)}{F_2(x,Q^2)} + \Delta A(g_1) = A_1^B(x) + \Delta A(g_1) \qquad (35)$$

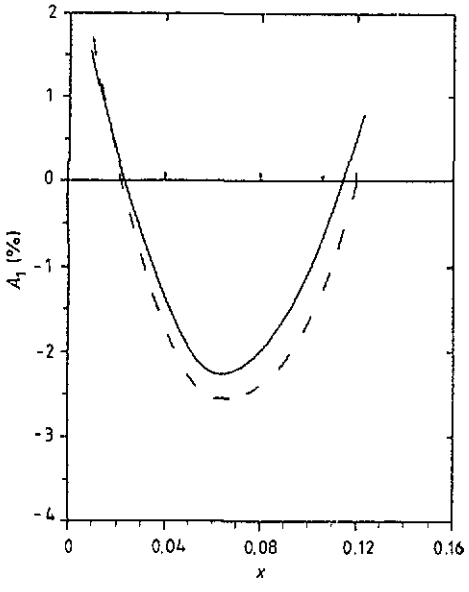

Figure 4. The x-dependence of the Born asymmetry (dashed line) and observed asymmetry (solid line) in the polarization muon–deuteron scattering for SMC kinematics. $E = 100\,\text{GeV}$. Longitudinally polarized target.

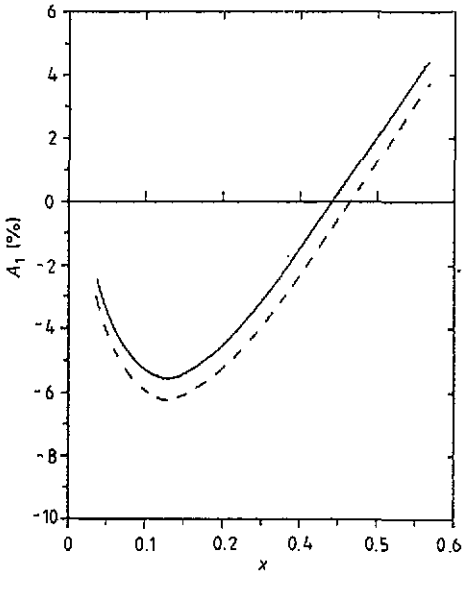

Figure 5. The x-dependence of the Born asymmetry (dashed line) and observed asymmetry (solid line) in the polarization electron–helium-3 scattering for SLAC kinematics. $E = 23\,\text{GeV}$. Longitudinally polarized target.

where ΔA is RC to the asymmetry. We start with the EMC data for the proton and the Schaefer model for the deuteron. SF $g_1(x)$ with fit parameters are specified on each step:

$$g_1^{(n)}(x) = \frac{F_2(x, Q^2)}{2x(1+R)}(A_m - \Delta A(g_1^{(n-1)})). \tag{36}$$

The procedure converges within 4 to 5 steps. As a result, we have extracted a $g_1(x)$ fit. Results of runs of POLRAD are collected in table 1. We demonstrated only the simplest variant of the iteration procedure. The availability of more abundant experimental data sets, for example, data for the spin asymmetry A_2, which contains SF $g_2(x)$, would furnish an opportunity to organize the iteration procedure for separating $g_1(x)$ and $g_2(x)$ contributions. Other variants are also possible.

(d) Procedure of radiative correction of experimental data. There are two versions for obtaining ΔA within the procedure of RC of experimental data. In the first case the correction $\Delta_1 A$ is obtained as a result of iteration procedure described above. In the second case it is

$$\Delta_2 A(x) = A_{\text{corr}}(g_1^{\text{model}}) - A_1^B(g_1^{\text{model}}(x)) \tag{37}$$

where $g_1(x)$ is calculated under a certain model and x is the kinematical point considered. SF g_1^{model} without argument in the first item indicates that it is used in the integrand of IRT. Here it is important to keep in mind the dependence of ΔA on the values of $g_1(x)$ used as the input. Extracting the dependence in the explicit form, we find by separating each cross section in (1) into the spin-average and the spin-dependent parts ($\sigma = \sigma^u + \sigma^p$)

$$\Delta A = \frac{\sigma_{\text{in}}^p(g_1) + \sigma_{\text{el}}^p + \sigma_{\text{q}}^p + \sigma_{\text{v}}^p}{D(\sigma_0^u + \sigma_{\text{in}}^u + \sigma_{\text{el}}^u + \sigma_{\text{v}}^u + \sigma_{\text{q}}^u)} - A_1^B(g_1(x))\frac{\sigma_{\text{in}}^u + \sigma_{\text{el}}^u + \sigma_{\text{v}}^u + \sigma_{\text{q}}^u}{\sigma_0^u + \sigma_{\text{in}}^u + \sigma_{\text{el}}^u + \sigma_{\text{v}}^u + \sigma_{\text{q}}^u}. \tag{38}$$

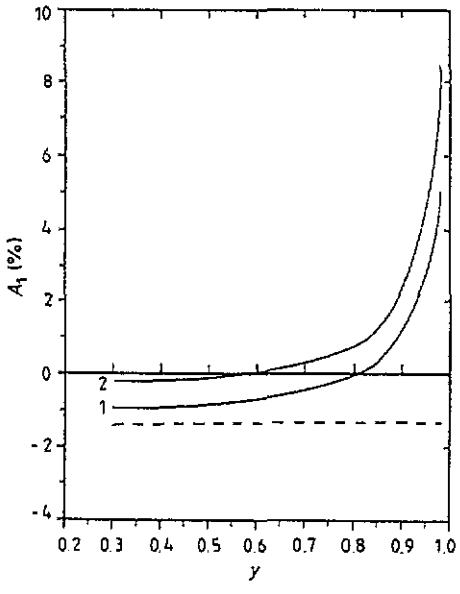

Figure 6. The y-dependence of the Born asymmetry (dashed line) and observed asymmetry (solid line, 1-for muons, 2-for electrons) in the polarization lepton–deuteron scattering. $E = 100\,\text{GeV}$ and $x = 0.1$. Longitudinally polarized target.

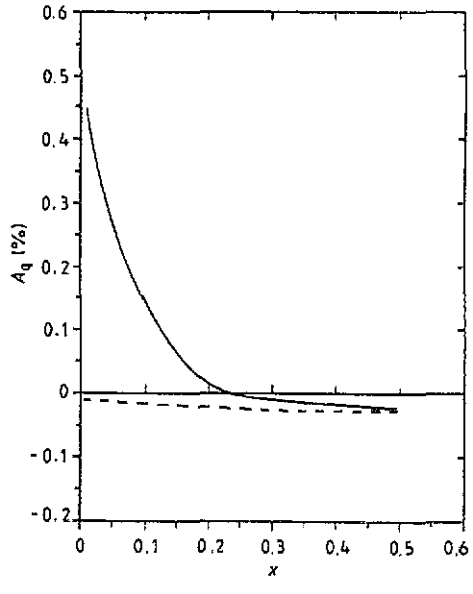

Figure 7. The quadrupole effects in the muon–deuteron scattering for SMC kinematics. Solid (dashed) line corresponds to the quadrupole asymmetry (Born asymmetry) with the account of RC.

Table 1. The results of the iteration procedure, $E = 100\,\text{GeV}$. A_m is the 'measured' spin asymmetry, A_{corr} is the radiatively corrected spin asymmetry. (a) proton data, (b) deuteron data.

(a)				(b)			
x	y	A_m (%)	A_{corr} (%)	x	y	A_m (%)	A_{corr} (%)
0.005	0.850	0.900	0.938	0.005	0.850	0.686	0.781
0.015	0.756	2.600	2.551	0.008	0.800	0.663	0.662
0.025	0.666	9.000	8.932	0.010	0.750	0.604	0.573
0.035	0.599	2.500	2.456	0.050	0.700	−1.352	−1.832
0.050	0.528	8.100	8.060	0.100	0.600	−1.061	−1.627
0.078	0.429	14.100	14.081	0.150	0.550	2.609	2.010
0.124	0.335	18.200	18.211	0.250	0.500	15.000	14.431
0.175	0.277	36.400	36.452	0.350	0.400	32.000	31.722
0.248	0.231	46.000	46.096	0.600	0.350	65.000	64.854
0.344	0.203	52.700	52.833	0.700	0.300	79.000	79.072
0.466	0.202	64.000	64.157	0.800	0.250	84.000	84.397
				0.900	0.250	68.000	68.313

The equality shows that there is an explicit linear dependence of ΔA on $g_1(x)$ (or A_1^B). From the existence of the dependence it transpires that the quantity ΔA calculated for $g_1(x)$ can be treated as correction only to Born asymmetry A_1^B, which is calculated for the same value of $g_1(x)$. However, this is far from being the case when we take up the second version of the RC procedure. The larger the difference between $g_1^{\text{model}}(x)$ and $g_1(x)$ obtained after the RC procedure, the rougher the calculation for ΔA. In the first version the extracted g_1

obeys equation (35) and hence, the difficulty is not apparent.

The uncertainty described is the main one for the second version of the RC procedure. Furthermore, we obtain the model-dependent correction and the use of different models can essentially change the correction. However, this is again due to a discrepancy between the values of SF $g_1(x)$ in the kinematical point considered.

In the first version we use for calculation the experimental data which have been processed. Large experimental errors (especially systematic errors) are the main uncertainty of the result obtained within the first version of the RC procedure. Another uncertainty originates from fitting: we need to choose the maximum degree of fitting polynomials. However, numerical analysis shows that the fitting uncertainty does not significantly influence the result.

In both versions it is necessary to extrapolate the model or the constructed fit into the entire kinematical plane. The choice of the procedure is ambiguous. In the article we extrapolate the asymmetry A_1^B over Q^2 and calculate $g_1(x, Q^2)$:

$$g_1(x, Q^2) = \frac{F_2(x, Q^2)}{2x(1 + R(x, Q^2))} A_1(x). \tag{39}$$

This is a simple way, which does not lead to contradictions ($A_1^B > 1$, $\sigma < 0 \ldots$) anywhere in the kinematical region.

We use the Schaefer model for g_1^p, g_1^n, convolution formulae for $g_1^d, g_1^{^3He}$ [39] and the experimental data: A_m^d from the SMC experiment [5] and $A_m^{^3He}$ from E142 at SLAC [6]. The first and second columns of table 2 give $\Delta_2 A$ and $\Delta_1 A$ after one step of iteration procedure. The better the description of the data by the model, the smaller the disagreement between the values for ΔA obtained in the two versions of the RC procedure. The third column shows how $\Delta_1 A$ varies with further steps of the iteration procedure. In the case of a deuteron target the corrections $\Delta_1 A$ obtained as a result of the iteration procedure and $\Delta_2 A$ even have opposite signs (see table 3). This is due to fact that the model $A_1^B(g_1(x))$ and the data A_m at the kinematical points have opposite signs.

Table 2. Radiative correction ΔA to electron–helium-3 DIS for SLAC kinematics under two versions of the RC procedure.

x	$\Delta_2 A$ (%)	$\Delta_1 A^{(0)}$ (%)	$\Delta_1 A$ (%)
0.035	2.072	1.275	1.482
0.050	1.732	1.376	1.570
0.078	1.451	1.623	1.812
0.124	1.234	1.984	2.189
0.175	1.054	2.164	2.369
0.248	0.871	2.133	2.312
0.344	0.677	1.620	1.838
0.466	0.415	0.886	0.948

In our opinion, the first version of the RC procedure, where fit for g_1 is constructed and used as input for ΔA calculation, is more suitable. The experimental error, which constitutes the main uncertainty in the iteration procedure, is large in the current experiments. But the iteration procedure of data processing will give unambiguous results when we have more precise data.

In the kinematical range of the polarization experiments considered, the radiative correction to the polarization asymmetry can be considerable and exceed 10%. The

Table 3. Radiative correction ΔA to muon–deuteron DIS for SMC kinematics under two versions of the RC procedure.

x	$\Delta_2 A$ (%)	$\Delta_1 A$ (%)
0.009	−0.213	0.528
0.015	−0.049	0.452
0.025	0.103	0.436
0.035	0.244	0.469
0.050	0.249	0.413
0.079	0.398	0.257
0.123	0.483	−0.029
0.173	0.502	−0.336
0.241	0.505	−0.557
0.343	0.416	−0.547
0.470	0.149	−0.032

correction becomes a leading contribution in the ranges where the Born polarization asymmetry tends to zero. Thus a numerical analysis of the total radiative correction, carryied out by using our FORTRAN program POLRAD, shows that a correct calculation of radiative effects is not only possible and desirable but absolutely essential for processing the experimental data supplied by polarization DIS.

Acknowledgements

The authors would like to thank V W Hughes, L Klostermann, G K Mallot, G Smirnov and R Windmolders for useful comments and discussions. We also thank N N Tarasenko for taking part in creating of the FORTRAN code POLRAD for the initial stage.

Appendix A

Here we consider polarization vectors for DIS of polarized leptons by polarized spin-1 or spin-1/2 nuclei:

$$\ell(k_1, \xi) + N(p, \eta) \to \ell(k_2) + X. \tag{A1}$$

In the lab frame $\eta = (n, 0)$ and n can be expanded as three components: n_{L} parallel to k_1, n_t normal to k_1 in the scattering plane (k_1, k_2), and $n_\perp$ normal to the scattering plane. If a target is polarized along $n_{\mathrm{L}}(n_t)$, then we speak about the longitudinal (transverse) polarization. In the third case we speak about the polarization being normal to scattering plane.

Let us build a basis in the four-dimensional space. The process of inclusive DIS is determined by three vectors of incoming (outgoing) leptons $k_1(k_2)$ and of incoming nuclei p which define a hyperplane in the four-dimensional space. We can choose the orthonormal basis system in this hyperplane $(p/M, \eta_{\mathrm{L}}, \eta_t)$, where

$$\begin{aligned} \eta_{\mathrm{L}} &= \lambda_s^{-1/2}\,(2Mk_1 - S/M\ p\,) \\ \eta_t &= \frac{(-SX + 2M^2Q_m^2))k_1 + \lambda_s k_2 - (SQ^2 + 2m^2S_x)p}{\lambda_s^{1/2}(SXQ^2 - m^2S_x^2 - M^2Q^4 - 4m^2M^2Q^2)^{1/2}}. \end{aligned} \tag{A2}$$

Invariants are defined in a standard manner:

$$\begin{aligned} &S = 2k_1 p \qquad X = 2k_2 p = (1-y)S \qquad Q^2 = -(k_1 - k_2)^2 = xyS \\ &S_x = S - X \qquad Q_m^2 = Q^2 + 2m^2 \qquad S_p = S + X \quad \lambda_s = S^2 - 4m^2 M^2. \end{aligned} \tag{A3}$$

Among all possible basis systems, our system differs from others in the following: two space-like vectors η_L and η_t in the lab frame are in the form $(n_{L,t}, 0)$, where $n_{L,t}$ are the above-considered three-dimensional polarization vectors. The basis vector system is uniquely fixed by this requirement. The basis in the four-dimensional space is produced by adding to the system an orthonormal to the hyperplane 4-momentum $\eta_\perp((n_\perp, 0)$ in the lab system). We have an expansion for any four-vector η:

$$\eta = \frac{\eta p}{M}\frac{p}{M} - (\eta\eta_L)\eta_L - (\eta\eta_t)\eta_t - (\eta\eta_\perp)\eta_\perp. \tag{A4}$$

If η is a polarization target vector, then for three above-mentioned cases we find: $\eta = \eta_L$ (longitudinally polarized target), $\eta = \eta_t$ (transversely polarized target), $\eta = \eta_\perp$ (target polarized orthogonally to the scattering plane).

The vector $\eta_\perp$ is orthogonal to all vectors determining the DIS (k_1, k_2, p), and hence it can appear in the expressions for the cross section in the form $\eta_\perp^2 = -1$ and only in the quadrupole part. Studying predominantly polarization asymmetry, we do not consider this effect in the article.

A scattered lepton is always longitudinally polarized (for the experiments considered). Using the expansion (A.4) for this vector, we obtain

$$\xi = \xi_L = \lambda_s^{-1/2}\left(\frac{S}{m}k_1 - 2mp\right). \tag{A5}$$

For the examination of the radiative effects, that is, for the processes of the type

$$\ell(k_1, \xi) + N(p, \eta) \to \ell(k_2) + \gamma(k) + X \tag{A6}$$

it is necessary to calculate the integrals over d^3k/k_0 from expressions, containing the scalar products of k and polarization vectors ξ and η. Since scalar products $k\xi$, $k\eta_L$, $k\eta_t$ are easily expressed in terms of invariants, this treatment allows us to eliminate the intricate and tedious procedure of tensor integration used in [16], and significantly simplifies the results. This is the most important advantage of the treatment considered.

Appendix B

In this appendix we choose an explicit form for the functions $\theta_{ij}(\tau)$, which are contained in the final formulae for the radiative tails. i runs from 1 to 8. This fact corresponds to the contributions of eight SF or form factor combinations and j runs from 1 to k_i which are

defined in (17).

$$\theta_{11}(\tau) = 4(Q^2 - 2m^2)F_{\rm IR}$$
$$\theta_{12}(\tau) = 4\tau F_{\rm IR}$$
$$\theta_{13}(\tau) = -4F - 2\tau^2 F_d$$
$$\theta_{21}(\tau) = 2(SX - M^2Q^2)F_{\rm IR}/M^2$$
$$\theta_{22}(\tau) = (2m^2 S_p F_{2-} + S_p S_x F_{1+} + 2(S_x - 2M^2\tau)F_{\rm IR} - \tau S_p^2 F_d)/2M^2$$
$$\theta_{23}(\tau) = (4M^2 F + (4m^2 + 2M^2\tau^2 - S_x\tau)F_d - S_p F_{1+})/2M^2$$
$$\theta_{31}(\tau) = -\frac{8P_{\rm L}m}{M}(\eta q k_2\xi - Q^2\xi\eta)F_{\rm IR}$$
$$\begin{aligned}\theta_{32}(\tau) = \frac{2P_{\rm L}m}{M}\,&(\eta\mathcal{K}(4m^2F_d^\xi - 4m^2F_{2+}^\xi + 2F_{\rm IR}^\xi - Q^2F_{2-}^\xi + Q_m^2F_{2+}^\xi)\\ &+k_2\xi(-8m^2F_d^\eta + 4m^2F_{2+}^\eta + 2\eta q\tau F_d) - 4\eta q F_{\rm IR}^\xi + 4\xi\eta\tau F_{\rm IR})\end{aligned} \tag{B1}$$
$$\begin{aligned}\theta_{33}(\tau) = \frac{2P_{\rm L}m}{M}&(\eta\mathcal{K}\tau(F_{2+}^\xi - F_{2-}^\xi - 2F_d^\xi)\\ &+2k_2\xi\tau F_d^\eta + 4m^2F_d^{\xi\eta} + 6F_{\rm IR}^{\xi\eta} + Q^2F_{2-}^{\xi\eta} - Q_m^2F_{2+}^{\xi\eta})\end{aligned}$$
$$\theta_{34}(\tau) = -\frac{2P_{\rm L}m\tau}{M}(2F_d^{\xi\eta} + F_{2+}^{\xi\eta} - F_{2-}^{\xi\eta})$$
$$\theta_{71}(\tau) = -2(Q^2 + 4m^2 + 12\eta k_1\eta k_2)F_{\rm IR}$$
$$\theta_{72}(\tau) = -2(3\eta\mathcal{K}(2m^2F_{2-}^\eta - \eta\mathcal{K}\tau F_d + \eta q F_{1+}) + 6\eta q F_{\rm IR}^\eta + \tau F_{\rm IR})$$
$$\theta_{73}(\tau) = 2F + \tau^2F_d + 6(\eta\mathcal{K}F_{1+}^\eta + \eta q\tau F_d^\eta - 4m^2F_d^{\eta\eta}).$$

For $i = 4$ and $i = 8$ we have:

$$\begin{aligned}&\theta_{i1}(\tau) = \eta q\bar\theta_{i1}(\tau)/M && \theta_{i2}(\tau) = (\eta q\bar\theta_{i2}(\tau) - \bar\theta_{i1}^\eta(\tau))/M\\ &\theta_{i3}(\tau) = (\eta q\bar\theta_{i3}(\tau) - \bar\theta_{i2}^\eta(\tau))/M && \theta_{44}(\tau) = (\eta q\bar\theta_{44}(\tau) - \bar\theta_{43}^\eta(\tau))/M\\ &\theta_{45}(\tau) = -\bar\theta_{44}^\eta(\tau)/M && \theta_{84}(\tau) = -\bar\theta_{83}^\eta(\tau)/M.\end{aligned} \tag{B2}$$

Here

$$\bar\theta_{41}(\tau) = \frac{4mP_{\rm L}}{M^2}(S_x\xi k_2 - 2\xi pQ^2)F_{\rm IR}$$
$$\begin{aligned}\bar\theta_{42}(\tau) = \frac{mP_{\rm L}}{M^2}&(4m^2(2k_2\xi F_d - k_2\xi F_{2+} - S_pF_d^\xi + S_pF_{2+}^\xi) - 2k_2\xi\tau S_xF_d\\ &-8\xi p\tau F_{\rm IR} + 2(2S_x - S_p)F_{\rm IR}^\xi + S_P(Q^2F_{2-}^\xi - Q_m^2F_{2+}^\xi))\end{aligned}$$
$$\begin{aligned}\bar\theta_{43}(\tau) = -\frac{mP_{\rm L}}{M^2}&(2F_d^\xi(2m^2 - \tau S_p) + 2k_2\xi\tau F_d + 6F_{\rm IR}^\xi\\ &+(Q^2 - \tau S_p)F_{2-}^\xi - (Q_m^2 - \tau S_p)F_{2+}^\xi)\end{aligned} \tag{B3}$$
$$\bar\theta_{44}(\tau) = \frac{mP_{\rm L}\tau}{M^2}(2F_d^\xi - F_{2-}^\xi + F_{2+}^\xi)$$
$$\bar\theta_{81}(\tau) = -\frac{6}{M}(S\eta k_2 + X\eta k_1)F_{\rm IR}$$
$$\begin{aligned}\bar\theta_{82}(\tau) = -\frac{3}{M}&(\eta\mathcal{K}(m^2F_{2-} - \tau S_pF_d) + \eta q F_{\rm IR} + m^2S_pF_{2-}^\eta\\ &+(S\eta k_1 + X\eta k_2)F_{1+} + 2S_xF_{\rm IR}^\eta)\end{aligned}$$
$$\bar\theta_{83}(\tau) = -\frac{3}{2M}(8m^2F_d^\eta - \eta\mathcal{K}F_{1+} - \eta q\tau F_d - S_x\tau F_d^\eta - S_pF_{1+}^\eta).$$

For $i = 5$ and $i = 6$ we have ($i' = i - 4$):

$$\begin{aligned}
\theta_{i1}(\tau) &= (Q^2 - 3(\eta q)^2)\theta_{i'1}(\tau)/M^2 \\
\theta_{i2}(\tau) &= ((Q^2 - 3(\eta q)^2)\theta_{i'2}(\tau) + 6\eta q\theta^{\eta}_{i'1}(\tau))/M^2 \\
\theta_{i3}(\tau) &= ((Q^2 - 3(\eta q)^2)\theta_{i'3}(\tau) + 6\eta q\theta^{\eta}_{i'2}(\tau) - 3\theta^{\eta\eta}_{i'1}(\tau))/M^2 \\
\theta_{i4}(\tau) &= (6\eta q\theta^{\eta}_{i'3}(\tau) - 3\theta^{\eta\eta}_{i'2}(\tau))/M^2 \\
\theta_{i5}(\tau) &= -3\theta^{\eta\eta}_{i'3}(\tau)/M^2
\end{aligned} \tag{B4}$$

where we introduced a vector $\mathcal{K} = k_1 + k_2$. Superscripts ξ or η in functions θ denote that labels must be added to all function F used in the corresponding θ. The functions F are the dependence of the the integral over z_1 and z_2, calculated analytically, on τ:

$$\begin{aligned}
F &= F(1) & F_d &= F\,(z_1^{-1}z_2^{-1}) = \tau^{-1}(F(z_2^{-1}) - F(z_1^{-1})) \\
F_{1+} &= F(z_2^{-1}) + F(z_1^{-1}) & F_{2+} &= F(z_2^{-2}) + F(z_1^{-2}) \\
F_{2-} &= F(z_2^{-2}) - F(z_1^{-2}) & F_{\mathrm{IR}} &= m^2F_{2+} - Q_m^2F_d.
\end{aligned} \tag{B5}$$

$F(A)$ is defined as

$$\int \frac{\mathrm{d}z}{\sqrt{R_{z_2}}}A = R^{\beta}F(A) \tag{B6}$$

where β is some number which is not defined since we are not interested here in the dependence on R. The functions F with superscripts are defined as

$$\begin{aligned}
\int \frac{\mathrm{d}z_2}{\sqrt{R_z}}Ak\xi &= R^{\beta}F^{\xi}(A) & \int \frac{\mathrm{d}z_2}{\sqrt{R_z}}Ak\eta &= R^{\beta}F^{\eta}(A) \\
\int \frac{\mathrm{d}z_2}{\sqrt{R_z}}Ak\xi k\eta &= R^{\beta}F^{\xi\eta}(A) & \int \frac{\mathrm{d}z_2}{\sqrt{R_z}}Ak\eta k\eta &= R^{\beta}F^{\eta\eta}(A).
\end{aligned} \tag{B7}$$

These functions are also reduced to scalars by using explicit forms of polarization vectors ξ and η (see appendix A):

$$\begin{aligned}
&F(z_2^{-1}) = C_2^{-1/2}(\tau) && F(z_1^{-1}) = C_1^{-1/2}(\tau) \\
&F(z_2^{-2}) = B_2(\tau)C_2^{-3/2}(\tau) && F(z_1^{-2}) = -B_1(\tau)C_1^{-3/2}(\tau) \\
&F(1) = \lambda_Q^{-1/2} && F(z_1) = -\lambda_Q^{-3/2}B_1(\tau) \quad F(z_1^2) = \tfrac{1}{2}\lambda_Q^{-5/2}(3B_1^2(\tau) - \lambda_Q C_1(\tau))
\end{aligned} \tag{B8}$$

where

$$\begin{aligned}
B_{1,2}(\tau) &= -\tfrac{1}{2}\,(\lambda_Q\tau \pm S_p(S_x\tau + 2Q^2)) \\
C_1(\tau) &= (S\tau + Q^2)^2 + 4m^2(Q^2 + \tau S_x - \tau^2M^2) \\
C_2(\tau) &= (X\tau - Q^2)^2 + 4m^2(Q^2 + \tau S_x - \tau^2M^2).
\end{aligned} \tag{B9}$$

References

[1] Ashman J *et al* 1989 *Nucl. Phys.* B **328** 1
[2] Ellis J and Jaffe R L 1974 *Phys. Rev.* D **9** 1444; 1974 *Phys. Rev.* D **10** 1669E
[3] Jaffe R L and Manohar A 1990 *Nucl. Phys.* B **337** 509
[4] Alguard M J *et al* 1976 *Phys. Rev. Lett.* **37** 1261; 1978 *Phys. Rev. Lett.* **41** 70
Baum G *et al* 1980 *Phys. Rev. Lett.* **45** 2000; 1983 *Phys. Rev. Lett.* **51** 1135
[5] Adeva B *et al* 1993 *Phys. Lett.* **302B** 533
[6] Anthony P L *et al* 1993 *Determination of the Neutron Structure Function* SLAC-PUB-6101
[7] Burkhardt H and Cottingham W N 1970 *Ann. Phys., NY* **56** 453
[8] Bjorken J D 1966 *Phys. Rev.* **148** 1467; 1970 *Phys. Rev.* D **1** 1376
[9] Technical design report 1993 *The HERMES collaboration* DESY-PRC 93/06, MPTI-V20-1993

[10] Vasiliev A N 1987 Polarization experiments at UNK *Proc. of the Workshop on the Experimental Program at UNK, Protvino* p 279
[11] Brock R, Brown S N, Montgomery H E and Corcoran M D FERMILAB-conf-90137
[12] Bardin D Yu and Shumeiko N M 1976 JINR P2-10113 (Dubna)
[13] Bardin D Yu and Shumeiko N M 1977 *Nucl. Phys.* B **127** 242
[14] Akhundov A A, Bardin D Yu and Shumeiko N M 1977 *Yad. Fiz.* **26** 1251; 1976 JINR E2-10147, JINR E2-10205 (Dubna)
[15] Shumeiko N M 1979 *Yad. Fiz.* **29** 1571
[16] Kukhto T V and Shumeiko N M 1982 *Yad. Fiz.* **36** 707; 1983 *Nucl. Phys.* B **219** 412
[17] Bailey J *et al* 1979 *Nucl. Phys.* B **151** 367
[18] Akhiezer A I, Sitenko A G and Tartakovsky V K 1989 *Nuclear Electrodynamics* (Kiev)
[19] Hofstadter R 1956 *Rev. Mod. Phys.* **28** 214
[20] de Forest T and Walecka J D 1966 *Adv. Phys.* **15** 1
[21] Lallena A M 1991 *Int. J. Mod. Phys.* A **6** 2213
[22] Stein S *et al* 1975 *Phys. Rev.* D **12** 1884
[23] Hoodbhoy P, Jaffe R L and Manohar A 1989 *Nucl. Phys.* B **312** 571
[24] Akushevich I V, Kukhto T V and Pacheco F 1992 *J. Phys. G: Nucl. Part. Phys.* **18** 1737
[25] Khachatryan G N and Shakhnazaryan Yu G 1977 *Yad. Fiz.* **26** 1258
[26] Sather E and Schmidt C 1990 *Phys. Rev.* D **42** 1424
[27] Choi S Y, Lee T and Song H S 1989 *Phys. Rev.* D **40** 2477
[28] Berkov A V, Nikitin Yu P and Terent'ev M V 1964 *Zh. Eksp. Teor. Fiz.* **46** 2202
Lapidus L I 1984 *Sov. J. Part. Nucl.* **15** 493
[29] Burkhardt H 1989 *NATO ASI Series* B **233** 201
[30] Gourdin M and Piketty C A 1964 *Nuovo Cimento* **32** 1136
[31] Muzafarov V M, Troitskii V E and Trubnikov S V 1983 *Sov. J. Part. Nucl.* **14** 1112
[32] Leidemann W, Lipparini E and Stringari S 1990 *Phys. Rev.* C **42** 416
[33] Yennie D R, Frautschi S C and Suura H 1961 *Ann. Phys.* **13** 379
[34] Akhundov A A, Bardin D Yu and Shumeiko N M 1977 *Yad. Fiz.* **26** 1251
[35] Brasse F W, Flauger W, Gauler J, Goel S P, Haidan R, Merkwitz M and Wriedt H 1976 *Nucl. Phys.* B **110** 413
[36] Amaudruz P *et al* 1992 *Phys. Lett.* **295B** 159
[37] Whitlow L W 1990 SLAC-report-357
[38] Arneodo M 1992 CERN-PPE/92-113
[39] Benesh S J and Vary J P 1991 *Phys. Rev.* C **44** 2175
[40] Schaefer A 1988 *Phys. Lett.* **208B** 175
[41] Woloshin R M 1989 *Nucl. Phys.* A **496** 749
[42] Close F E and Kumano S 1990 *Phys. Rev.* D **42** 2377
[43] Khan H and Hoodbhoy P 1991 *Phys. Rev.* C **44** 1219
[44] Schiff L I 1964 *Phys. Rev.* B **133** 802
[45] Bilen'kaya S I, Lapidus L I, Bilen'kii S M, Kazarinov Yu M 1974 *Zh. Eksp. Teor. Fiz. Pis'ma* **19** 613
[46] Bernabeu J and Pascual P 1972 *Nuovo Cimento* A **10** 61
Bernabeu J 1972 *Nucl. Phys.* B **49** 186
[47] Moniz E J 1969 *Phys. Rev.* **184** 1154